OPEN

Ultra-Low-Field Portable MRI and Extracorporeal Membrane Oxygenation: Preclinical Safety Testing

Jin Kook Kang, MD[1]

Eric Etchill, MD[1]

Kate Verdi, MD[1]

Ana K. Velez, MD[1]

Sean Kearney, BS[1]

Jeffrey Dodd-o, MD[2]

Errol Bush, MD[3]

Samantha By, PhD[4]

Eddy Boskamp, PhD[4]

Christopher Wilcox, DO, MS[1]

Chun Woo Choi, MD[1]

Bo Soo Kim, MD[1,5]

Glenn J. R. Whitman, MD[1]

Sung-Min Cho, DO, MHS[1,6]

CONTEXT: Conventional MRI is incompatible with extracorporeal membrane oxygenation (ECMO) cannulas and pumps. Ultra-low-field portable MRI (ULF-pMRI) with 0.064 Tesla may provide a solution, but its safety and compatibility is unknown.

HYPOTHESIS: ULF-pMRI does not cause significant displacement and heating of ECMO cannulas and does not affect ECMO pump function.

METHODS AND MODELS: ECMO cannulas in various sizes were tested ex vivo using phantom models to assess displacement force and heating according to the American Society for Testing and Materials criteria. ECMO pump function was assessed by pump flow and power consumption. In vivo studies involved five female domestic pigs (20–42 kg) undergoing different ECMO configurations (peripheral and central cannulation) and types of cannulas with an imaging protocol consisting of T2-weighted, T1-weighted, FLuid-Attenuated Inversion Recovery, and diffusion-weighted imaging sequences.

RESULTS: Phantom models demonstrated that ECMO cannulas, both single lumen with various sizes (15–24-Fr) and double lumen cannula, had average displacement force less than gravitational force within 5 gauss safety line of ULF-pMRI and temperature changes less than 1°C over 15 minutes of scanning and ECMO pump maintained stable flow and power consumption immediately outside of the 5 gauss line. All pig models showed no visible motion due to displacement force or heating of the cannulas. ECMO flow and the animals' hemodynamic status maintained stability, with no changes greater than 10%, respectively.

INTERPRETATION AND CONCLUSIONS: ULF-pMRI is safe and feasible for use with standard ECMO configurations, supporting its clinical application as a neuroimaging modality in ECMO patients.

Extracorporeal membrane oxygenation (ECMO) is a rescue therapy increasingly used in patients with refractory cardiac and respiratory failure (1). Unfortunately, ECMO patients are at considerable risk of acute brain injury (ABI), which is associated with two- to three-fold increase in mortality (2, 3). Standardized neuromonitoring, including CT, electroencephalography, transcranial Doppler ultrasound, somatosensory evoked potentials, and near-infrared spectroscopy, can improve ABI detection and potentially improve neurologic outcomes at discharge, highlighting the importance of early identification and appropriate intervention in these cases (4, 5).

Brain CT is a valuable imaging modality for assessing ABI. However, it falls short in detection of early ischemic brain injury, especially in the posterior circulatory region (6). Since ECMO patients often have cardiopulmonary instability, transporting these patients to radiology suite is challenging and dangerous as it may lead to adverse events up to 20% and requires highly trained staff to be present during transportation (7). Although portable CT may

KEY POINTS

Question: Does ultra-low-field portable MRI (ULF-pMRI) maintain safety and compatibility with extra-corporeal membrane oxygenation (ECMO) system in phantom and in vivo pig models?

Findings: Our phantom and in vivo pig models demonstrated that ECMO cannulas and pumps did not undergo any significant displacement force or heating when tested with a 0.064 Tesla ULF-pMRI demonstrating the safety and feasibility of ULF-pMRI with ECMO equipment.

Meaning: ULF-pMRI can be safely used with ECMO, suggesting its potential as an effective neuroimaging tool in critical care settings to improve diagnosis and outcomes for ECMO patients.

eliminate any transportation-related problems, radiation exposure and the low sensitivity for diagnosing acute ischemic injury remain issues (8). MRI, in contrast, is a gold standard for ABI diagnosis with a better sensitivity than CT, especially for detecting acute ischemic stroke (9, 10). However, conventional MRI operates at high-strength magnetic fields (1.5–3 T) in strict, access-controlled environments, making ECMO devices (cannula and pump), incompatible.

The recent development of ultra-low-field portable MRI (ULF-pMRI) technology has enabled the acquisition of clinically meaningful imaging with ferromagnetic materials in much closer proximity to the system than a conventional MR would allow. ULF-pMRI (64 mT, approximately 1/23 the field strength of a conventional MRI) provides a 5 gauss line (defined as the access-controlled zone and denoting the border within which the magnetic field could affect implanted devices) that is only about 2.5 feet from the center of the scanner (11). Sheth et al (11) demonstrated the feasibility of an ULF-pMRI in an ICU setting in non-ECMO neurocritically ill patients without significant adverse events or complications. Furthermore, its capacity for close bedside monitoring of hemodynamically labile patients presents a promising application in ECMO settings.

As ECMO cannulas are typically positioned within the 5 gauss line of ULF-pMRI, the ferromagnetic properties of the tip and/or coils of wire inside the ECMO cannula could potentially result in static displacement and heating, which raises safety concerns. Additionally, although the ECMO pump is located outside of the 5 gauss line of ULF-pMRI, its function could be potentially impacted by the fringe magnetic field. To date, comprehensive safety evaluations of ECMO cannulas and pumps under ULF-pMRI conditions have not been documented. We hypothesize that ECMO cannulas do not experience substantial displacement force or heating and that the ECMO pump function remains unaffected. The aim of this study was to assess our hypotheses in both phantom and in vivo pig models.

MATERIALS AND METHODS

This study was approved by Johns Hopkins University Animal Care and Use Committee under protocol number SW21M451 (Investigation of mechanisms of end-organ injury during extracorporeal membrane oxygenation, approved in January 11, 2022). All animal handling and procedures were conducted in strict compliance with the National Institutes of Health (Bethesda, MD) guidelines for the humane treatment of animals. As this study involved phantom and animal models and not human subjects, Institutional Review Board approval was not applicable.

This study used the 64-mT Swoop Portable MR Imaging system (Hyperfine, Guilford, CT; hardware versions 1.6, 1.7, and 1.8). The Swoop system is an Food and Drug Administration (FDA)-cleared device, with its initial clearance for brain imaging in patients aged two and up received in February 2020 (U.S. FDA K192002), and an expanded clearance for all patient ages received in August 2020 (U.S. FDA K201722). This was an investigator-initiated study supported by a research services agreement between Johns Hopkins University and Hyperfine, Samantha By, PhD, and Eddy Boskamp, PhD, were employees of Hyperfine at the time and contributed to the investigation, particularly for these preclinical studies. These studies were performed after the FDAs approval of the Swoop system.

The 5 gauss line of an MRI machine defines the border within which the magnetic field could affect implanted devices. Established test methods were used to identify potential major hazards to the

patient due to displacement forces or radiofrequency-induced heating from components related to ECMO (American Society for Testing and Materials [ASTM] F2052 [12] and F2182 [13]). **Supplemental Table 1** (http://links.lww.com/CCX/B423) presents risks associated with the use of ECMO in ULF-pMRI and the safety evaluations performed in this study. Specifically, we used established standards (ASTM F2503-13 [14] and International Organization for Standardization/Technical Committee [ISO/TS] 10974 Ed2 [15]) as guidelines to evaluate the safety of ECMO cannulas located inside the 5 gauss line and the proper function of an ECMO pump located outside of the 5 gauss line of ULF-pMRI.

Displacement Force

ASTM F2052 (Test Method for Measurement of Magnetically Induced Displacement Force on Medical Devices) was used to evaluate the displacement force (12). The magnitude of the force on a device (F) is measured as $F = mg\tan(\alpha)$, where m is the mass of the device, g is acceleration due to gravity (9.81 m/s^2), and α is the angular deflection, which represents the displacement force exerted on the ECMO cannula. According to the ASTM F2052, if the mean value for α is less than 45°, the magnetically induced displacement force is less than the force on the device due to gravity (its weight) and is considered safe.

Four cannulas, all of which have wire-reinforced tips, were evaluated: 1) 15-Fr Maquet cannula (outer diameter: 5.0 mm, effective insertion length: 15 cm, overall length: 30 cm, weight: 10.8 g), 2) 16-Fr Edwards cannula (outer diameter: 5.3 mm, effective insertion length: 15 cm, overall length: 24 cm, weight: 9.4 g), 3) 24-Fr Edwards Aortic cannula (outer diameter:12.0 mm, overall length: 37.6 cm, effective insertion length: 19 cm, weight: 31.1 g), and 4) double lumen cannula (weight: 38.6 g).

For each cannula, a nonmagnetic mechanical fixture was constructed to measure the force on the cannula. The mechanical fixture included a plastic spring gauge, which measured the displacement of the cannula. The spring gauge was connected to the tip of the cannula via a spring-and-pulley system. This mechanical fixture was placed on the patient bridge as shown in **Supplemental Figure 1** (http://links.lww.com/CCX/B423). Force values were calculated based on the

characterization of the plastic spring. At the lowest setting on the mechanical fixture, the cannula was slowly moved into the bore until the cannula was deflected and just in contact with the scanner surface (location 1). The cannula was moved further into the bore until the cannula was no longer in contact with the scanner surface (location 2). The highest magnetic force was approximated as the center of the two locations.

Two force values were measured: maximum and neutral. The "maximum" force was defined as the force required to pull the cannula from the surface of the magnet cover (**Supplemental Fig. 2A**, http://links.lww.com/CCX/B423) to a neutral position. This would represent the worst-case scenario and is not physically possible given that the cannula would be inside the patient. The "neutral" force was defined as the force required to pull the cannula from a position that mimics where it would be inside a patient during an ULF-pMRI examination to its neutral position without any effects from a magnetic field. This force represents a more realistic scenario (**Supplemental Fig. 2B**, http://links.lww.com/CCX/B423). The spring gauge was used to measure the deflection force on the cannula in the two setups mentioned above; the spring gauge was used to pull the cannula until it was completely level (**Supplemental Fig. 2C**, http://links.lww.com/CCX/B423). The average value of these two forces was compared with the force on the cannula due to gravity.

Heating

ASTM F2182 (Standard Test Method for Measurement of Radio Frequency Induced Heating on or Near Passive Implants During MRI) was used to test heating, which suggests that temperature change less than 2°C over 15 minutes of magnetic resonance exposure is considered safe.

Three cannulas, all of which have wire-reinforced tips, were evaluated: 1) 15-Fr Maquet cannula (outer diameter: 5.0 mm, insertion length: 15 cm), 2) 24-Fr Edwards Aortic cannula (outer diameter: 8.0 mm, overall length: 37.6 cm), and 3) double lumen cannula. A gelled-saline phantom inside an acrylic phantom was constructed (**Supplemental Fig. 3**, http://links.lww.com/CCX/B423). The gelled-saline phantom was made using 1.32 g/L sodium chloride and 10 g/L partial sodium salt of polyacrylic acid in distilled water. The conductivity of the phantom

was 0.44 S/m at 18.9°C. A Rugged Fiber Optic Temperature Monitoring system (H201-04, four channels, FOS-TG-02-T-00-000 fiber optic probes with standard standard tip connector) was used. The fiber optic probes were connected to the metallic tips of the cannulas. A fiber optic probe was placed in the phantom away from any metallic objects as a baseline reference measurement. All measurements were performed on a Swoop system (hardware version 1.6; Hyperfine, Guilford, CT) with software version RC8.1.1. A T2-weighted sequence (Echo time = 209.2 ms, Repetition time = 2000 ms, echo train length = 80, scan time: 5:54 min) was repeated three times. Temperature measurements were logged from each channel at a temporal resolution of 1 seconds.

ECMO Pump Malfunction

The function of a Biomedicus centrifugal pump (Medtronic, Eden Prairie, MN) and Sarns 8000 roller pump (Sams; Terumo CVS, Ann Arbor, MI) was tested to ensure that ULF-pMRI did not cause any pump malfunction. A saline phantom was used, and pump flow was monitored using LabView (Austin, TX) according to the testing method developed by ISO/TS 10974 Ed2 (15). To assess if the pump function would be affected by ULF-pMRI, pump flows were measured in two different configurations: 1) pump on (positioned just outside the 5 gauss line) and ULF-pMRI on and 2) pump on (positioned several meters away from the 5 gauss line) and ULF-pMRI off. Less than 10% change in pump flow was considered safe. Additionally, a Kill-A-Watt tool (P3 International, New York, NY) was used to measure the power consumption of the centrifugal pump in both configurations in three different pump flow settings (1, 2, and 6 L/min).

Large Animal Experiment: Pig Model

After the phantom experiments, we performed large animal experiments using five pigs with various ECMO cannula configuration, sizes, and locations (**Table 1**). Centrifugal and roller pumps, blenders, control panels, and oxygenators were also tested to ensure proper functionality assessed by evaluation of pump flow. For each study, a baseline, pre-cannulation scan—T2-weighted, FLuid-Attenuated Inversion Recovery (FLAIR), T1-weighted, and DWI on ULF-pMRI—was

performed. Examples of the in vivo experimental setup for pigs with ECMO cannulation undergoing ULF-pMRI are shown in **Figure 1**. ECMO flow, vital signs, and temperature were continuously monitored throughout the scanning process.

We defined that less than 10% change in mean arterial pressure (MAP), less than 10% decrease in ECMO flow, and less than 10% decrease in peripheral oxygen saturation in pigs during scanning processes were considered safe and stable.

RESULTS

Phantom Experiments

Displacement Force. For all four cannulas (24-Fr, 16-Fr, 15-Fr, and double lumen), the neutral and maximum displacement forces, as well as their average, across five measurements were less than the force due to gravity of the cannula (**Table 2**), which meets the safety criteria suggested by ASTM F2052.

Heating. For three cannulas in different sizes (24-Fr, 15-Fr, and double lumen), the measured temperature change during 15 minutes of scanning was less than 1°C, which meets the safety criteria suggested by ASTM F2182 (**Table 3**).

ECMO Malfunction. For both the centrifugal and roller pumps, pump flow changes in configuration 1 (pump on, positioned just outside the 5 gauss line, and ULF-pMRI on) were less than 10% compared with that of configuration 2 (pump on, positioned several meters away from the 5 gauss line, and ULF-pMRI off), meeting the criteria. For the centrifugal pump, the average difference in power consumption between two configurations across five different measurements was minimal, with less than 1 W at all three pump settings (1, 2, and 6 L/min). **Figure 2** demonstrates consistent pump flows during the scanning process for both pumps.

Large Animal Experiment: Pig Model

Five female domestic pigs (20–42 kg) were anesthetized using a combination of ketamine 4.5 mg/kg, xylazine 88 µg/kg, and telazol 1.1 mg/kg via intramuscular injection. Pigs underwent endotracheal intubation, were maintained under inhaled isoflurane 0.5–2.0%, and were mechanically ventilated with 100% oxygen. Once anesthesia and monitoring were established, ultrasound-guided percutaneous access to the bilateral

TABLE 1.
Summary of Pig Model Experiments

Experiment No.	Weight (kg)	Pump Type	Cannulation Settings	Protocol Details
1	40	Roller pump	Peripheral cannulation: left femoral artery: 8-Fr and right femoral vein: 10-Fr	Baseline MRI performed
			Peripheral cannulation: left femoral artery: 18-Fr and right femoral vein: 19-Fr	MRI performed for each configuration
			Neck cannulation: left femoral artery: 18-Fr, right femoral vein: 19-Fr, and jugular vein: 21-Fr	
			Central cannulation: left femoral artery: 18-Fr, right femoral vein: 19-Fr, aorta: 20-Fr, and right atrium: 32-Fr dual stage	
2	40	Centrifugal pump	Peripheral cannulation: left femoral artery: 18-Fr and right femoral vein: 19-Fr	Baseline MRI performed
			Neck cannulation: left femoral artery: 18-Fr, right femoral vein: 19-Fr, and jugular vein: 21-Fr	MRI performed for each configuration
			Central cannulation: left femoral artery: 18-Fr, right femoral vein: 19-Fr, aorta: 20-Fr, and right atrium: 32-Fr dual stage	
3	22	Roller pump	Peripheral cannulation: left femoral artery: 16-Fr and right femoral vein: 19-Fr	Baseline MRI performed
				Ventricular fibrillation induced, then ECMO initiated
				MRI performed while on ECMO
4	20	Centrifugal pump	Peripheral cannulation: left femoral artery: 16-Fr and right femoral vein: 21-Fr	No baseline MRI performed
				Ventricular fibrillation induced, then ECMO initiated
				ECMO, MRI performed while on ECMO
5	42	Centrifugal pump	Neck cannulation: right jugular vein: 24-Fr double lumen crescent	Baseline MRI performed
				MRI performed while on ECMO

ECMO = extracorporeal membrane oxygenation.

femoral arteries and veins were obtained. Two vascular sheaths (5-Fr) were placed in a contralateral femoral artery and vein for transducing systemic blood pressure, administering fluids and medications, and drawing blood.

Then, one of the following two techniques were performed to achieve peripheral or central cannulation. 1) For peripheral cannulation, systemic heparin (100 U/kg) were administered. ECMO cannula in various sizes were placed in contralateral femoral vessels under ultrasound guidance. For peripheral jugular ECMO cannulation, a cutdown on the neck was to identify jugular vein. Venotomy was performed to place the venous cannula. 2) For central cannulation, a median sternotomy was performed to place arterial cannula in the ascending aorta and venous cannula in the right atrium. After cannulation, flow was initiated, and vital signs were closely monitored. In total, we performed: 1) baseline scan prior to placement of any cannulas (T2-weighted, FLAIR, T1-weighted, and
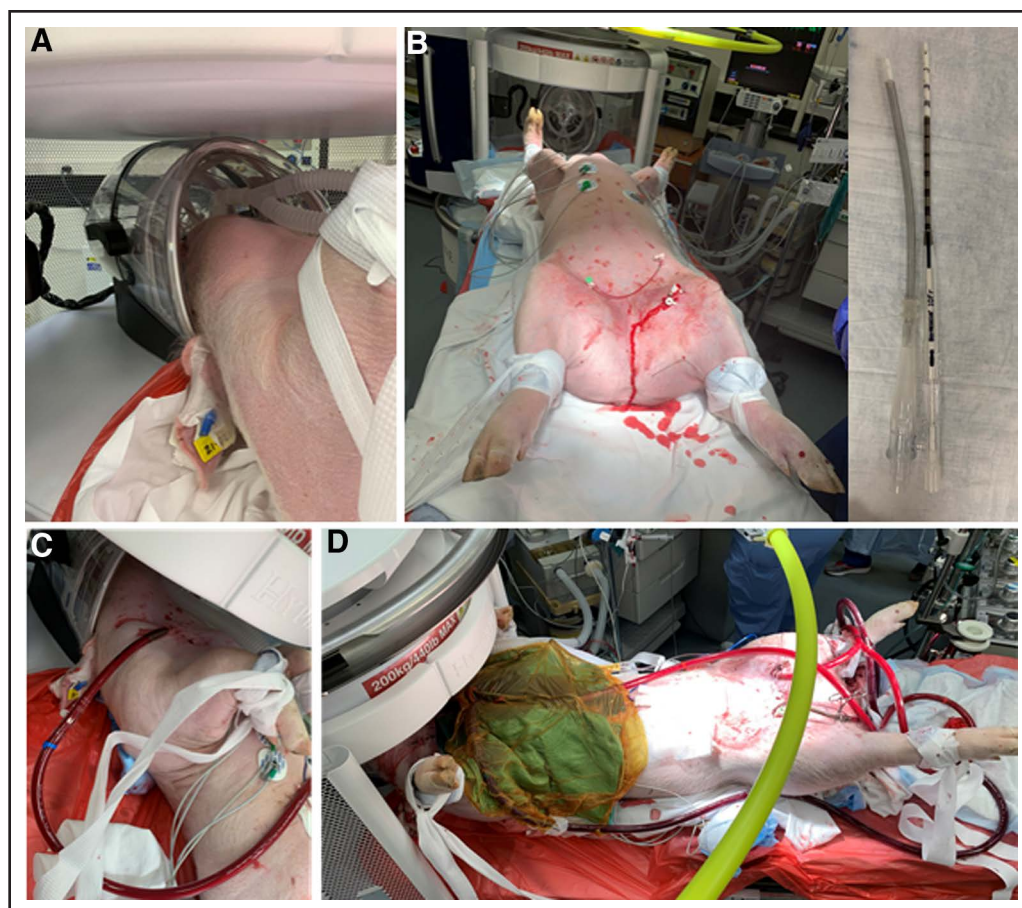
Figure 1. Various setups for testing compatibility of extracorporeal membrane oxygenation with Swoop including a baseline scan with no cannula insertion (**A**), peripheral insertion with the smaller cannulas (**B**), neck insertion (**C**), and central insertion with pacing wires (**D**).

change. Additionally, compared with the baseline imaging, there were no artifacts in images obtained after ECMO cannulation.

DISCUSSION

We evaluated the compatibility and safety of the ULF-pMRI with ECMO cannulas and pumps routinely used in the clinical setting in patients. Because of the ferromagnetic components, wire-reinforced cannulas can potentially undergo displacement force and heating in an MR environment. The highest temperature change is expected at the tip of a long metallic wire (16), and tip heating is dramatically increased when the wire length meets a resonance condition with the radiofrequency excitation applied during an MR examination. For example, the half-wavelength of a conducting wire in vivo is theoretically 215 mm at conventional MR setting of 1.5 T (assuming a relative permittivity of 600), which is on the order of the length of ECMO cannulas. Previously, only ECMO cannulas that are not reinforced with wires have been tested in the conventional MR setting (1.5 T) because of this (17). As the risk of displacement decreases with reduced magnetic field strength and the half-wavelength of a conductive wire in vivo is estimated to be 1244 mm at 64 mT, we hypothesized that the potential for these safety issues would be greatly reduced or eliminated for the ULF-pMRI system. In our ex vivo phantom experiments, the ECMO cannulas did not experience any significant displacement force or heating when placed within the 5 gauss line of the ULF-pMRI system within the ASTM safety guidelines, demonstrating that ULF-pMRI is safe and compatible with these ECMO cannulas.

DWI on ULF-pMRI), 2) scan with femoral cannulas in place (peripheral ECMO), 3) scan with femoral and neck cannulas in place (peripheral ECMO), and 4) scan with central cannulas in place (Fig. 1). ECMO flow, vital signs, and temperature were continuously monitored throughout the experiments. Temperature changes of the animals were also monitored via FLIR ONE Pro camera (FLIR Systems, Wilsonville, OR).

During all scanning processes of the five pigs, no visible motion or radiofrequency-induced heating more than 1°C of the ECMO cannulas was observed, irrespective of if they were within (neck cannulation) or beyond the 5 gauss line (femoral cannulation). Images were obtained via thermal camera to qualitatively evaluate the temperature change of the pigs with ECMO cannulation (**Supplemental Fig. 4**, http://links.lww.com/CCX/B423). In all pigs during scanning processes, MAP and oxygen saturation remained stable with minimal changes less than 10%. ECMO flow was consistently maintained with less than 10% flow

TABLE 2.

Displacement Calculated Forces Over Five Measurements for Different Cannulas (Neutral Force, Maximum Force)

Measurement	24-Fr	16-Fr	15-Fr	Double Lumen
1	0.041–0.074 N	0.008–0.019 N	0.03–0.041 N	0.063–0.118 N
2	0.041–0.063 N	0.008–0.019 N	0.03–0.041 N	0.063–0.118 N
3	0.041–0.063 N	0.008–0.019 N	0.03–0.041 N	0.063–0.118 N
4	0.041–0.063 N	0.008–0.019 N	0.03–0.041 N	0.063–0.118 N
5	0.041–0.063 N	0.008–0.019 N	0.03–0.041 N	0.063–0.118 N
Average	0.041–0.065 N	0.008–0.019 N	0.03–0.041 N	0.063–0.118 N
Force due to gravity	0.31 N	0.09 N	0.11 N	0.38 N

TABLE 3.

Measured Temperature Change

Device	Temperature Change (°C)
Baseline	0.2°C
24-Fr cannula	0.1°C
15-Fr cannula	0.2°C
Double lumen cannula	0.2°C
American Society for Testing and Materials standard	1°C

Our phantom model, based on the safety recommendations developed by the ASTM, was also assessed pump function when located just outside the 5 gauss line of the ULF-pMRI, where it would be placed in clinical practice. For both centrifugal and roller pumps, there were minimal differences in pump flow compared with the baseline measurements taken when the pumps were positioned several meters beyond the 5 gauss line and while the ULF-pMRI was not in use. These results are consistent with a study testing a portable ECMO system placed just outside the 200-gauss line of a 1.5 T MR system (17). Additionally, given the predominant use of the centrifugal pump in clinical settings, we specifically evaluated its power consumption across three different flow rates (1, 2, and 6 L/min), which showed negligible difference in power consumption across all settings tested. These results suggest that ECMO pump function, when placed just outside the 5 gauss line, is unaffected by ULF-pMRI. Based on these findings, different types and brands of ECMO machine/pump are expected to maintain proper function during scanning process.

Furthermore, our in vivo experiments using pig models further corroborated the safety and compatibility of ULF-pMRI. In all five pig models, ECMO cannulas did not undergo any visible displacement or heating. Additionally, none exhibited a change in MAP of greater than 10%, a decrease in ECMO flow of greater than 10%, and a decrease in peripheral oxygen saturation of more than 10% throughout the scanning processes. Notably, adult patients would likely be positioned farther from the scanner than the pig models described in this study. This increased distance from the ULF-pMRI further ensures the safety of the ECMO cannulas in real clinical settings. Important to note, our study did not evaluate the quality and adequacy of the brain imaging in pigs because ULF-pMRI was primarily designed for human brain evaluation. There is a further need to investigate and validate the quality of those images and strategies to mitigate ECMO-associated ABI using ULF-pMRI in clinical setting in a prospective multicenter study.

Our study has several limitations. Although our phantom and validation studies were designed to closely emulate real-life clinical settings, they inherently cannot capture the full complexity of an actual patient in critical care environment. Our study did not evaluate every component of ECMO (membrane oxygenator and heat exchanger); however, the risk of malfunction of those devices is minimal since they are outside of 5 gauss. Every commercially available ECMO cannula in different sizes, length, and manufactures were not evaluated as such evaluation would be impractical.
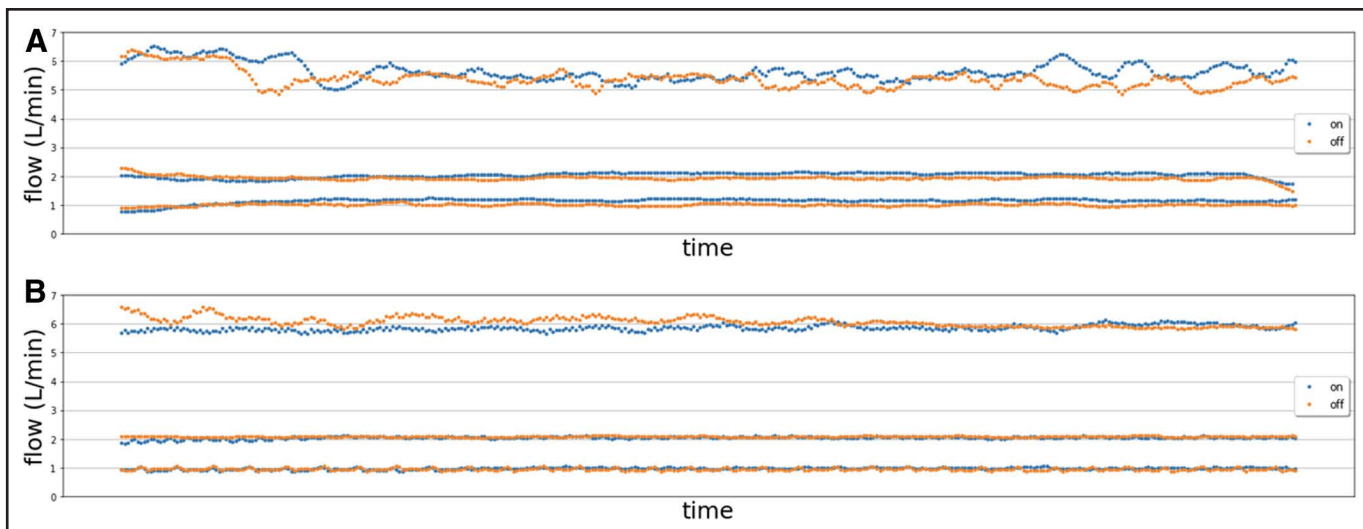
Figure 2. Pump flow changes during the scanning process for Biomedicus centrifugal pump (**A**) and Sarns 8000 roller pump (**B**) with ultra-low-field portable MRI on (*blue*) and off (*red*).

CONCLUSIONS

We demonstrated the safety and compatibility of ULF-pMRI with the ECMO cannulas and pumps based on the ASTM criteria with phantom and animal models. This highlights the potential role of ULF-pMRI as a valuable and safe point-of-care neuroimaging tool to facilitate prompt diagnosis of ABI and potentially improve outcomes in ECMO patients. Multicenter prospective research is necessary to assess the effectiveness and validity of ULF-pMRI in clinical practice.

ACKNOWLEDGMENTS

We want to extend our gratitude to Lori Arlinghaus, PhD, for her invaluable contributions in reviewing this article.

1 Division of Cardiac Surgery, Department of Surgery, Johns Hopkins Hospital, Baltimore, MD.

2 Division of Cardiac Anesthesiology, Department of Anesthesiology and Critical Care Medicine, Johns Hopkins University School of Medicine, Baltimore, MD.

3 Division of Thoracic Surgery, Department of Surgery, Johns Hopkins Hospital, Baltimore, MD.

4 Hyperfine, Inc., Guilford, CT.

5 Division of Pulmonary and Critical Care Medicine, Department of Medicine, Johns Hopkins University School of Medicine, Baltimore, MD.

6 Division of Neurosciences Critical Care, Department of Neurology, Neurosurgery, Anesthesiology and Critical Care Medicine, Johns Hopkins Hospital, Baltimore, MD.

REFERENCES

1. McCarthy FH, McDermott KM, Kini V, et al: Trends in U.S. extracorporeal membrane oxygenation use and outcomes: 2002-2012. *Semin Thorac Cardiovasc Surg* 2015; 27:81–88

2. Cho S-M, Canner J, Caturegli G, et al: Risk factors of ischemic and hemorrhagic strokes during venovenous extracorporeal membrane oxygenation: Analysis of data from the extracorporeal life support organization registry. *Crit Care Med* 2021; 49:91–101

3. Cho S-M, Canner J, Chiarini G, et al: Modifiable risk factors and mortality from ischemic and hemorrhagic strokes in patients receiving venoarterial extracorporeal membrane oxygenation: Results from the extracorporeal life support organization registry. *Crit Care Med* 2020; 48:e897–e905

4. Cho S-M, Ziai W, Mayasi Y, et al: Noninvasive neurological monitoring in extracorporeal membrane oxygenation. *ASAIO J* 2020; 66:388–393

5. Ong CS, Etchill E, Dong J, et al: Neuromonitoring detects brain injury in patients receiving extracorporeal membrane oxygenation support. *J Thorac Cardiovasc Surg* 2023; 165:2104–2110.e1

6. Hwang DY, Silva GS, Furie KL, et al: Comparative sensitivity of computed tomography vs. magnetic resonance imaging for

detecting acute posterior fossa infarct. *J Emerg Med* 2012; 42:559–565

7. Ericsson A, Frenckner B, Broman LM: Adverse events during inter-hospital transports on extracorporeal membrane oxygenation. *Prehosp Emerg Care* 2017; 21:448–455

8. Rumboldt Z, Huda W, All JW: Review of portable CT with assessment of a dedicated head CT scanner. *AJNR Am J Neuroradiol* 2009; 30:1630–1636

9. Chalela JA, Kidwell CS, Nentwich LM, et al: Magnetic resonance imaging and computed tomography in emergency assessment of patients with suspected acute stroke: A prospective comparison. *Lancet* 2007; 369:293–298

10. Kidwell CS, Chalela JA, Saver JL, et al: Comparison of MRI and CT for detection of acute intracerebral hemorrhage. *JAMA* 2004; 292:1823–1830

11. Sheth KN, Mazurek MH, Yuen MM, et al: Assessment of brain injury using portable, low-field magnetic resonance imaging at the bedside of critically ill patients. *JAMA Neurol* 2021; 78:41

12. ASTM International: F04 Committee: Test Method for Measurement of Magnetically Induced Displacement Force on Medical Devices in the Magnetic Resonance Environment. 2022. Available at: https://www.astm.org/f2052-21.html. Accessed November 8, 2023

13. ASTM International: F04 Committee: Test Method for Measurement of Radio Frequency Induced Heating On or Near Passive Implants During Magnetic Resonance Imaging. 2022. Available at: https://www.astm.org/f2052-21.html. Accessed November 8, 2023

14. ASTM International: F04 Committee: Practice for Marking Medical Devices and Other Items for Safety in the Magnetic Resonance Environment. 2022. Available at: https://www.astm.org/f2052-21.html. Accessed November 8, 2023

15. ISO/TS 10974:2018(en): Assessment of the Safety of Magnetic Resonance Imaging for Patients With an Active Implantable Medical Device. 2018. Available at: https://www.iso.org/obp/ui/#iso:std:iso:ts:10974:ed-2:v1:en. Accessed November 8, 2023

16. Yeung CJ, Susil RC, Atalar E: RF safety of wires in interventional MRI: Using a safety index. *Magn Reson Med* 2002; 47:187–193

17. Lidegran MK, Frenckner BP, Mosskin M, et al: MRI of the brain and thorax during extracorporeal membrane oxygenation: Preliminary report from a pig model. *ASAIO J* 2006; 52:104–109